2015

Modeling of minimum void ratio for sand–silt mixtures

Ching S. Chang
University of Massachusetts Amherst

Jia-Yi Wang
National Taiwan University of Science and Technology

Louis Ge
National Taiwan University of Science and Technology

Recommended Citation

Chang, Ching S.; Wang, Jia-Yi; and Ge, Louis, "Modeling of minimum void ratio for sand–silt mixtures" (2015). *Engineering Geology*. 849.
https://doi.org/10.1016/j.enggeo.2015.07.015

Engineering Geology 196 (2015) 293–304

Contents lists available at ScienceDirect

Engineering Geology

journal homepage: www.elsevier.com/locate/enggeo

Modeling of minimum void ratio for sand–silt mixtures

Ching S. Chang [a], Jia-Yi Wang [b], Louis Ge [b,*]

[a] Department of Civil and Environmental Engineering, University of Massachusetts, Amherst, MA 01002-1111, United States
[b] Department of Civil Engineering, National Taiwan University, Taipei 10617, Taiwan

ARTICLE INFO

Article history:
Received 28 January 2015
Received in revised form 11 July 2015
Accepted 16 July 2015
Available online 30 July 2015

Keywords:
Void ratio
Packing density
Soil mixture

ABSTRACT

Minimum void ratio or maximum packing density is an important soil property in geotechnical engineering. It correlates to the volume change tendency, the pore fluid conductivity, and the shear strength of the soil. In geotechnical engineering, it often requires to estimate the minimum void ratio for a sand–silt mixture with any amount of fines content, based only on few laboratory test results. The minimum void ratio for soil mixtures is usually estimated by methods based on, to some extent, an empirical approach, for example, the AASHTO coarse particle correction method. In this paper, based on a more fundamental approach using the concept of dominant particle network, we aim to develop a mathematical model that can predict the minimum void ratio for sand–silt mixtures with any amount of fines content. The developed model only requires two parameters for the prediction of minimum void ratios of soil mixtures with various fines contents. The developed model is evaluated by the experimental results on 33 types of soil mixtures available in the literature, including mixtures of sands (Ottawa sand, Nevada sand, Toyoura sand, Hokksund sand, etc), and silts (ATC silt, Nevada fines, crushed silica fines, grind Toyoura fines, etc). Comparisons of the results are discussed.

1. Introduction

Granular soil is a packing of soil particles of different sizes. Research on soil mechanics, for several decades, revealed that the amount of fines in a sand–silt mixture has significant effects on its mechanical properties (e.g. Selig and Ladd, 1973; Aberg, 1992; Miura et al., 1997; Cubrinovski and Ishihara, 2002; Bobei et al., 2009; Peters and Berney, 2010; Fuggle et al., 2014). This is not surprising because how particles are packed is greatly influenced by the particle size distribution, which is an important factor governing the properties of materials. The importance of particle size distribution has also been observed in many branches of industry, such as ceramic processing (Reed, 1995), powder metallurgy (Smith, 2003), and concrete mixes (Powers, 1968).

Studies of packing density as a function of particle size distribution were meager published around 1930s. Research interest of high-density packing of ceramics and metal particles was renewed around 1954, for the reason of impetus of atomic energy and space research. However, the research works were mainly considering packing of uranium oxide and optimum particle size distribution (PSD) for maximum packing density (McGeary, 1961). For soils, a method of prediction of maximum packing density of soil with different sizes of particles was proposed by Humphres (1957) using an empirical and graphical method. Around 1986, AASHTO T 224-86 specifications postulate an empirical method for estimating the maximum packing density by using a "correction factor" for coarse particles that can be applied when the percent of gravel size particles is less than or equal to 70%. Kezdi (1979) outlined an analytical method to estimate the minimum porosity of a binary mixture of granular soils. The method is based on the ideal situation that the pore space among large particles is fully filled by the fine particles without alternating the packing structure of large particles. Thus, the method is applicable only to very small size of fine particles and often overestimates the maximum packing density. For improving compaction control of granular fill, Fragaszy and Sneider (1991) carried out an extensive set of experiments on soils with a wide range of particle sizes, and compared the measured maximum dry density with the two empirically based predictive methods: "Humphres method (Humphres, 1957)" and "AASHTO correction factor" method (AASHTO, 1986). In association with the liquefaction potential of silty-sand, Lade et al. (1998) had carried out minimum void ratio tests for different types of soil mixtures. They also proposed an analytical method for predicting the minimum void ratio for spheres with different sizes; however, this method is applicable only to an ideal situation that the small particles are much smaller than the large ones. Vallejo (2001) measured porosities on mixtures of two different sizes of glass beads. He also proposed an equation with similar form to the method by Kezdi (1979) for estimating the porosity of the binary mixtures. He indicated that the theoretical minimum porosity was very difficult to achieve in laboratory mixtures. Cubrinovski and Ishihara (2002) examined a large number of test data on silty-sand and presented a set of empirical equations to show the influence of fines content on the magnitude of minimum void ratio. Apart from these studies, computer simulation analyses using discrete element method have also been

* Corresponding author.
E-mail addresses: chang@ecs.umass.edu (C.S. Chang), r02521134@ntu.edu.tw (J.-Y. Wang), louisge@ntu.edu.tw (L. Ge).

http://dx.doi.org/10.1016/j.enggeo.2015.07.015
0013-7952/

implemented to study the characteristics of the void ratio of particle mixtures (An, 2013; Fuggle et al., 2014). The trend of computer simulation results resembles that obtained from experimental tests. Nevertheless, these methods are not yet capable of predicting the minimum void ratio for sand–silt mixtures.

A more extensive research on analytical method has been carried out in the field of concrete mixes by de Larrard (1999) that can be used to predict packing density of concrete mixes of aggregate and sand. This method has been widely used for concrete mixture design to optimize the packing densities of cement, mortar and concrete (e.g. Kwan and Fung, 2009; Fennis et al., 2013). Methods similar to the formulation by de Larrard (1999) can also be found in the field of powder mixes by Stovall et al. (1986) and Yu and Standish (1987), which are commonly used in the pharmaceutical industry.

However, the applicability of these existing analytical methods (similar to that given by de Larrard, 1999) has not yet been examined for the packing density of sand–silt mixtures with different particle sizes. In this study, the existing packing model by de Larrard (1999) is evaluated by comparing the measured and predicted minimum void ratios for a number of silt–sand mixtures. Deficiencies of the existing packing models are identified, and a new model is proposed that can better predict the minimum void ratios for sand–silt mixtures with different particle sizes.

2. Existing packing theories and models

The minimum void ratio is 0.35 for a hexagonal packing of monosize spheres. The minimum void ratio for a randomly arranged packing is about 0.56–0.66. The particle shape has noteworthy influence on the value of minimum void ratio, which is generally lower for more spherical particles and higher for less spherical (or more angular) particles. When it comes to a packing of particles with different sizes, the minimum void ratio is also governed by the particle size distribution. Considering the simplest case of a binary mixture of particles with two sizes, the experimental results on steel shot mixtures given by McGeary (1961) are illustrated in Fig. 1. The packing density is plotted for large particles of 3.14 mm mixed with six other sizes (i.e., 0.91, 0.66, 0.48, 0.28, 0.19, and 0.16 mm). This figure shows the characteristics of packing density change due to fines content.

When the fines content is low, the smaller particles would fill the voids among the larger particles and thereby increase the packing density. Upon an increase of fines content, the voids among the large particles are eventually fully occupied and thereby the maximum packing density is reached. As the fines content continues to increase, the reverse trend is observed (i.e., the packing density decreases). The decrease of packing density is due to the fact that large particles are pushed apart by the small particles. As the fines content increases further, eventually the volume of small particles becomes much greater than that of large particles, and the larger particles would present as isolated inclusions embedded within the network of the smaller particles. Hence, as shown in Fig. 1, mixing particles of two different sizes would in general have a greater packing density than packing with one particle size.

The experimental results in Fig. 1 also show that the relative size of the large and small particles is an important factor influencing the packing density. It is obvious that, in order for the small particles to be fit into the voids between large particles, the small particles should be relatively smaller than the large particles. For a packing of spheres, the size of small particles should be at least 6.5 times smaller of the large particle size in order to fit in the tetrahedral cavities of the sphere packing. The effect of relative particle size on the packing density was shown by McGear and replotted in Fig. 2 for fines content of 24%. The packing density increases (or the void ratio decreases) significantly for particle size ratio less than 7. Larger than this value, the packing efficiency decreases rapidly.

To cater for multiple mixes of different size particles, the above binary packing model has been extended to a variety of packing models, most of which are based on the linear packing theory (Westman and Hugill, 1930) and may thus be classified as linear packing models. The linear packing theory postulates that for the multiple components (each comprising of all the particles of a certain size) mixed together, the change of packing density is a linear combination of the two mechanisms: (1) the inserted small particles fill voids of the packing, and (2) the inserted large particles embedded in the matrix of the packing. In the early age theory, the particle size ratio was not considered. In the 1980s, this theory has been refined to account for the effect of particle size ratio by Stovall et al. (1986), Yu and Standish (1987), and de Larrard (1999).

The packing density equations proposed in the afore-mentioned packing density models have the same expression. The equation in terms of the notation given by de Larrard (1999) is as follows

$$\gamma_i = \frac{\beta_i}{1-\sum_{j=1}^{i-1}[1-\beta_i+w(r)\beta_i(1-1/\beta_j)]y_j-\sum_{j=i+1}^{n}[1-l(r)\beta_i/\beta_j]y_j} \quad (1)$$

where γ_i is the predicted packing density of a mixture consisting of n components. It requires the input of the packing density of each component and the solid volumetric fraction of each component (i.e. particle size distribution). Considering component i is dominant, β_i and β_j are the packing densities of components i and j, y_i is the solid volumetric fraction of component j, r is the size ratio between the components i and j, and $l(r)$ and $w(r)$ are the interaction functions accounting for the effects of particle size ratio. The two functions are termed as "loosening function" and "wall function", respectively.

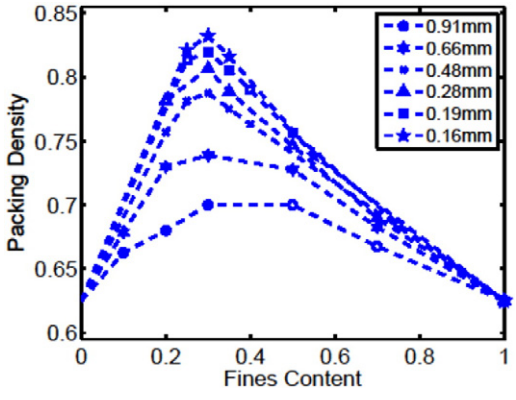

Fig. 1. Binary packing of steel shots.
Data from McGeary (1961).

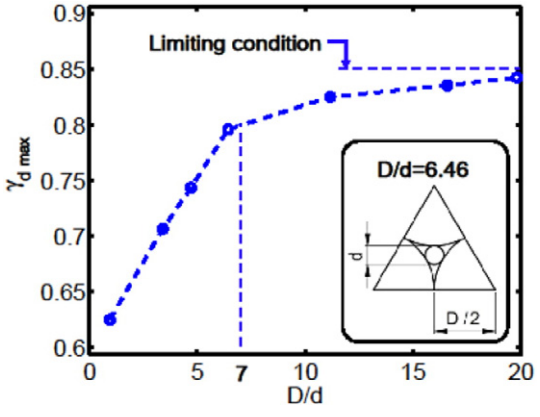

Fig. 2. Effect of particle size ratio on maximum packing density.
Data from McGeary (1961).

Although the packing density equations were same for the aforementioned models, the interaction functions are not quite the same for different packing models. In this study, the most advanced and popular packing model by de Larrard (1999) is employed for packing density prediction. In this model, the interaction functions accounting for the particle interactions between component i and component j are given by:

$$l(r) = \sqrt{1-(1-r)^{1.02}} \tag{2}$$

$$w(r) = 1-(1-r)^{1.5}. \tag{3}$$

More mathematical details of the packing model can be found in the original references.

3. Evaluation of the existing model

De Larrard (1999) developed his model for concrete mixes based on experimental results obtained from round to sub-round aggregates with size ranging from sand to gravel. Yu and Standish (1987) developed their model for powder processing using the data from Ben Aim and Le Goff (1967) for packing of perfect spheres. Here we consider the material of sand–silt mixture, which is commonly encountered in geotechnical engineering. We are interested in knowing whether the predictability of the existing models is suitable for sand–silt mixture. For this purpose, a large set of data for sand–silt mixtures is selected to evaluate the applicability of these models. The selected experimental results of sand–silt mixtures and their references are listed in Table 1. For each mixture, the values of pertinent property are also listed. Instead of maximum packing density γ_{max} commonly used in concrete mixes, we list minimum void ratio e_{min}. There is a direct relationship between maximum packing density and minimum void ratio given by $\gamma_{max} = 1/(1 + e_{min})$.

The minimum void ratio depends on inherent properties of the soil such as the fines content, grain size distribution, grain shapes and the method of deposition (Cho et al., 2006; Yilmaz et al., 2008). There is no applicable ASTM procedure for determining minimum void ratio over the entire range of fines content. Test methods specified in ASTM D 4254 standards are applicable to soils that may contain up to 15% fines content. Most test results shown in Table 1 were carried out according to ASTM D 4254 standards, even for specimens having fines content greater than 15%. Several other methods of determining the values of minimum void ratio were also used for the soil mixtures listed in Table 1: Japanese test standard, ASTM standard, and methods employed by Kolbuszewski (1948), Mulilis et al. (1977), and Vaid and

Table 1
Selected experimental results of sand–silt mixtures and their references.

Sand/silt mixture	D_{50} (mm)	d_{50} (mm)	d_{50}/D_{50}	e (sand)	e (silt)	a_{12}	b_{12}	Slope a	Slope b	ψ_s	ψ_s
Ottawa F55-crushed silica (R1)	0.25	0.01	0.0400	0.615	0.634	0.727	0.79	−1.1689	0.5049	Round to subround	Angular
Ottawa 50/200-Nevada fines (R2)	0.202	0.05	0.2475	0.548	0.754	0.5	0.55	−0.6710	0.5074	Angular	Angular
Ottawa F95-Nevada fines (R2)	0.163	0.05	0.3067	0.580	0.754	0.18	0.3	−0.1417	0.3480	Subround	Angular
Ottawa C109-Silica fines (R3)	0.39	0.012	0.0308	0.500	1.800	0.84	0.89	−1.0520	1.7450	Subround	
Ottawa C109-Kaolinite (R3)	0.39	0.0012	0.0031	0.500	0.600	0.99	0.89	−1.4840	0.5450	Subround	
Foundry (R4)	0.25	0.01	0.0400	0.608	0.627	0.725	0.796	−1.1606	0.5030	Round to subround	Angular
Nevada sand-ATC silt (R5)	0.14	0.036	0.2571	0.642	0.877	0.382	0.467	−0.4820	0.5348	Subangular	Angular
Nevada 50/200-Nevada fines (R2)	0.14	0.044	0.3098	0.570	0.754	0.24	0.32	−0.2370	0.3664	Subangular	Angular
Nevada 50/80-Nevada fines (R6)	0.211	0.05	0.2370	0.581	0.754	0.43	0.64	−0.5812	0.5448	Subangular to angular	
Nevada 80/200-Nevada fines (R6)	0.12	0.05	0.4167	0.617	0.754	0.15	0.2	−0.1261	0.2604	Subangular to angular	
Nevada 50/80-Nevada 80/200 + fine (R6)	0.1655	0.05	0.3021	0.581	0.754	0.29	0.32	−0.3357	0.3589	Subangular to angular	
Toyoura (R7)	0.17	0.01	0.0588	0.591	0.609	0.443	0.229	−0.6948	0.1533	Elongated subangular	Angular
Hokksund (R8)	0.45	0.035	0.0778	0.570	0.760	0.534	0.714	−0.7498	0.5970	Sharp edges, cubical	Angular, subangular
MGM (R9)	0.116	0.009	0.0776	0.755	1.000	0.38	0.724	−0.5150	0.7916	Highly angular to subround	Thin and plate-like
Vietnam (R10)	0.16	0.023	0.1438	0.607	0.596	0.544	0.678	−0.8792	0.4005	Subangular	Subangular
Cambria-Nevada fines (R6)	1.5	0.05	0.0333	0.538	0.754	0.65	0.82	−0.9241	0.6572	Round	Angular
Ottawa C109-Silica sand (R3)	0.39	0.15	0.3846	0.500	0.425	0.42	0.2	−0.6735	0.0250	Subround	Subround
Vietnam (R10)	0.37	0.16	0.4324	0.552	0.583	0.096	0.242	−0.1210	0.1649	Subangular	Subangular
Cambria-Nevada 50/80 (R6)	1.5	0.211	0.1407	0.538	0.581	0.45	0.57	−0.6685	0.3497	Round	Subangular
Cambria-Nevada 80/200 (R6)	1.5	0.12	0.0800	0.538	0.624	0.48	0.59	−0.6933	0.4038	Round	Angular
Nevada 50/80-Nevada 80/200 (R6)	0.211	0.12	0.5687	0.581	0.617	0.08	0.06	−0.0934	0.0709	Subangular to angular	
Silica #16–#18 #16–#18 (R11)	1.08	1.08	1.0000	0.633	0.633	0	0	0.0000	0.0000	Subangular	
Silica #16–#18 #18–#30 (R11)	1.08	0.78	0.7222	0.633	0.615	0.03	0.035	−0.0668	0.0038		
Silica #16–#18 #30–#50 (R11)	1.08	0.4	0.3704	0.633	0.644	0.42	0.35	−0.6797	0.2325		
Silica #16–#18 #30–#80 (R11)	1.08	0.42	0.3889	0.633	0.590	0.41	0.36	−0.6952	0.1847		
Silica #16–#18 #50–#80 (R11)	1.08	0.263	0.2435	0.633	0.696	0.53	0.5	−0.8363	0.3792		
Silica #16–#18 #80–#100 (R11)	1.08	0.167	0.1546	0.633	0.682	0.67	0.74	−1.0784	0.5170		
Silica #16–#18 #80–#120 (R11)	1.08	0.137	0.1269	0.633	0.697	0.69	0.75	−1.1074	0.5383		
Silica #16–#18 #80–#200 (R11)	1.08	0.103	0.0954	0.633	0.651	0.84	0.74	−1.3692	0.4862		
Silica #16–#18 #100–#120 (R11)	1.08	0.137	0.1269	0.633	0.697	0.88	0.738	−1.4297	0.5307		
Silica #16–#18 #100–#200 (R11)	1.08	0.103	0.0954	0.633	0.668	0.89	0.81	−1.4499	0.5472		
Silica #16–#18 #120–#200 (R11)	1.08	0.097	0.0898	0.633	0.682	0.71	0.72	−1.1456	0.5043		
Silica #16–#18 #200–#400 (R11)	1.08	0.057	0.0528	0.633	0.700	0.9	0.94	−1.4633	0.6620		

R1 Thevanayagam (2007).
R2 Lade and Yamamuro (1997).
R3 Pitman et al. (1994).
R4 Thevanayagam et al. (2002).
R5 Yamamuro and Covert (2001).
R6 Lade et al. (1998).
R7 Zlatovic and Ishihara (1997).
R8 Yang (2004).
R9 Fourie and Papageorgiou (2001).
R10 Cho (2014).
R11 Yilmaz (2009).

Negussey (1988). It is noted that, although values of the minimum void ratios are somewhat different, depending on the methods employed, the trend does not vary.

Fig. 3 shows the comparison of measured and predicted results for all the sand–silt mixtures listed in Table 1. The predicted values were computed using Eqs. (1) to (3). Comparisons of the predicted and measured packing density values are plotted on the left side of Fig. 3. In general, the prediction is higher than the measured value and the scatter range is up to 20%. The values of packing density were then converted to their equivalent values of void ratio, and the comparisons in terms of void ratio values are plotted on the right side of Fig. 3. It is noted that, in terms of void ratio, the scatter range increases significantly, which is up to 50%. The increase of scatter is due to the fact that the relationship between packing density and void ratio is not linear. Therefore, it may be misleading to look at the comparisons based on the variable of packing density.

The packing densities computed using Eqs. (1) to (3) as a function of fines content are shown in Fig. 4 for some typical soil mixtures listed in Table 1. The calculated trend of packing density compares well with that of measured results. However, the magnitude of calculated packing density is higher than the measured ones, especially at the range between 0.2–0.5 fines contents. The degree of discrepancies varies from mixture to mixture.

The comparison shows that the predictability of the model for concrete mixes or industrial material is not suitable for sand–silt mixtures.

4. Development of a new model

In soil mechanics, the void ratio e is more commonly used instead of packing density. The void ratio is defined as the ratio of the void volume V_v to the solid volume V_s. In order to see the relationship between minimum void ratio and fines content for soil mixtures, we converted the measured packing densities in Fig. 4 into minimum void ratios. And the converted data were plotted in Fig. 5. The dash lines in Fig. 5 were fitted from the measured minimum void ratios. Observed from Figs. 4 and 5, the relationship between void ratio and fines content seems to be more linear, as compared to the relationship between packing density and fines content. Thus, a model using void ratio as variable is more preferable than using packing density.

A simple modeling concept of "dominant network" for a packing with two-size particles has been proposed by Chang and Meidani (2013). On this basis, a new model is developed herein for the analysis of minimum void ratio. The derivation is described in the following section.

For a binary packing consisting of two components; component 1 is coarse particles and component 2 is fine particles. The particle sizes of the two components are denoted as d_1 and d_2, the volume of solids is denoted as V_{s1} for coarse particles and as V_{s2} for fine particles. Their respective solid volume fractions are y_1 and y_2 ($y_1 + y_2 = 1$). The minimum void ratios for the two components are e_1 and e_2. Our objective is to estimate the minimum void ratio of the binary mixture packing.

First, we consider the coarse particle as the dominant material. The phase diagram of a pure sand packing is shown in Fig. 6a. Then we consider the mixture of silt and sand. In a limiting situation, all the added silt particles fill into the voids among the sand particles without altering the network of coarse particles. Thus the solid volume of silt (S2) occupies a space in the void volume (V1) and the total volume remains constant (see Fig. 6b).

However, in a general case (see Fig. 6c), during the process of achieving minimum void ratio of the soil mixture, the structure of coarse particles is usually distorted and the change of total volume is denoted as ΔV. The void volume of the sand–silt mixture is V_v. The change of void volume is defined as $\Delta V_v = V_v - V_{v1}$. Since $V_v = V_{v1} + \Delta V - V_{s2}$ (see Fig. 6c). Thus the change of void volume can be expressed as $\Delta V_v = \Delta V - V_{s2}$. For the limiting case, $\Delta V = 0$ and the change of void volume $\Delta V_v = -V_{s2}$.

The minimum void ratio e^M of the mixture shown in Fig. 6c can be expressed as

$$e^M = \frac{V_v}{V_{s1} + V_{s2}} = \frac{V_{v1} + \Delta V_v}{V_{s1} + V_{s2}}. \tag{4}$$

Compared this void ratio of mixture e^M with the void ratio of pure sand e_1, the void ratio decreases by two factors: (1) void volume is decreased due to filling phenomenon; (2) solid volume is increased to $V_{s1} + V_{s2}$. In Chang and Meidani (2013), the change of void volume is assumed to be proportional to the amount of silt added in the mixture, i.e., $\Delta V_v = aV_{s2}$, where a is a material constant. Note that the limit of 'a' is -1 corresponding to the limiting situation where no change of total volume has occurred. For convenience, we replaced 'a' by another constant $\tilde{a}$ thus the assumption is $\Delta V_v = aV_{s2}$, where $\tilde{a} = a + 1$, so that $\tilde{a} = 0$ is corresponding to the limiting condition. Using this assumption, e^M in Eq. (4) can be written as a function containing e_1 and y_2:

$$e^M = e_1(1-y_2) - y_2 + \tilde{a}y_2. \tag{5}$$

Comparing this model with that for concrete mixes (e.g. de Larrard, 1999), the major difference is on the assumptions of volume change due to the filling phenomenon. For example, the method by de Larrard is in terms of packing density (or solid volume fraction), and de Larrard assumed that, due to the filling phenomenon, the packing density is changed. The change of packing density is proportional to a compound variable, which is a multiplication of solid volume-fraction of the fine grains and the original solid volume-fraction of the coarse grains. In the present model, the assumption is that the void volume change is proportional to the amount of fines in the mixture. Thus, the proportional constant in de Larrard's model does not carry the same physical meaning as that in the present model.

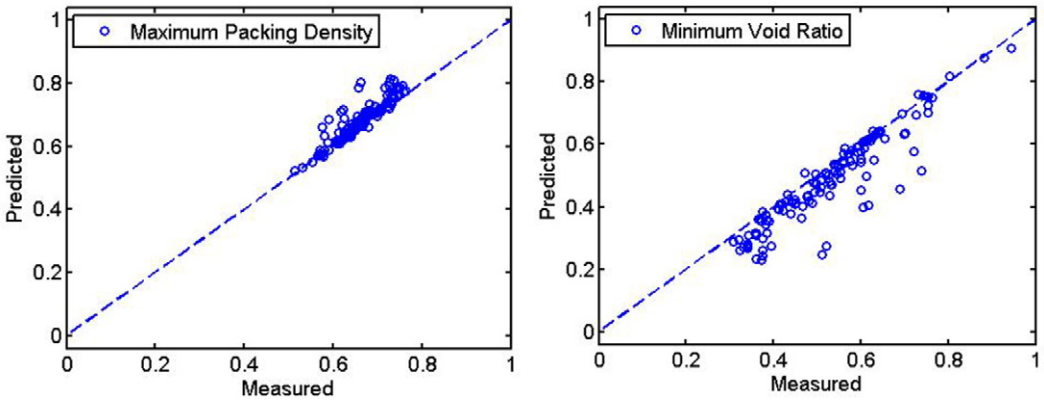

Fig. 3. Comparison between predicted and measured packing densities/void ratios using Eqs. (1) to (3).

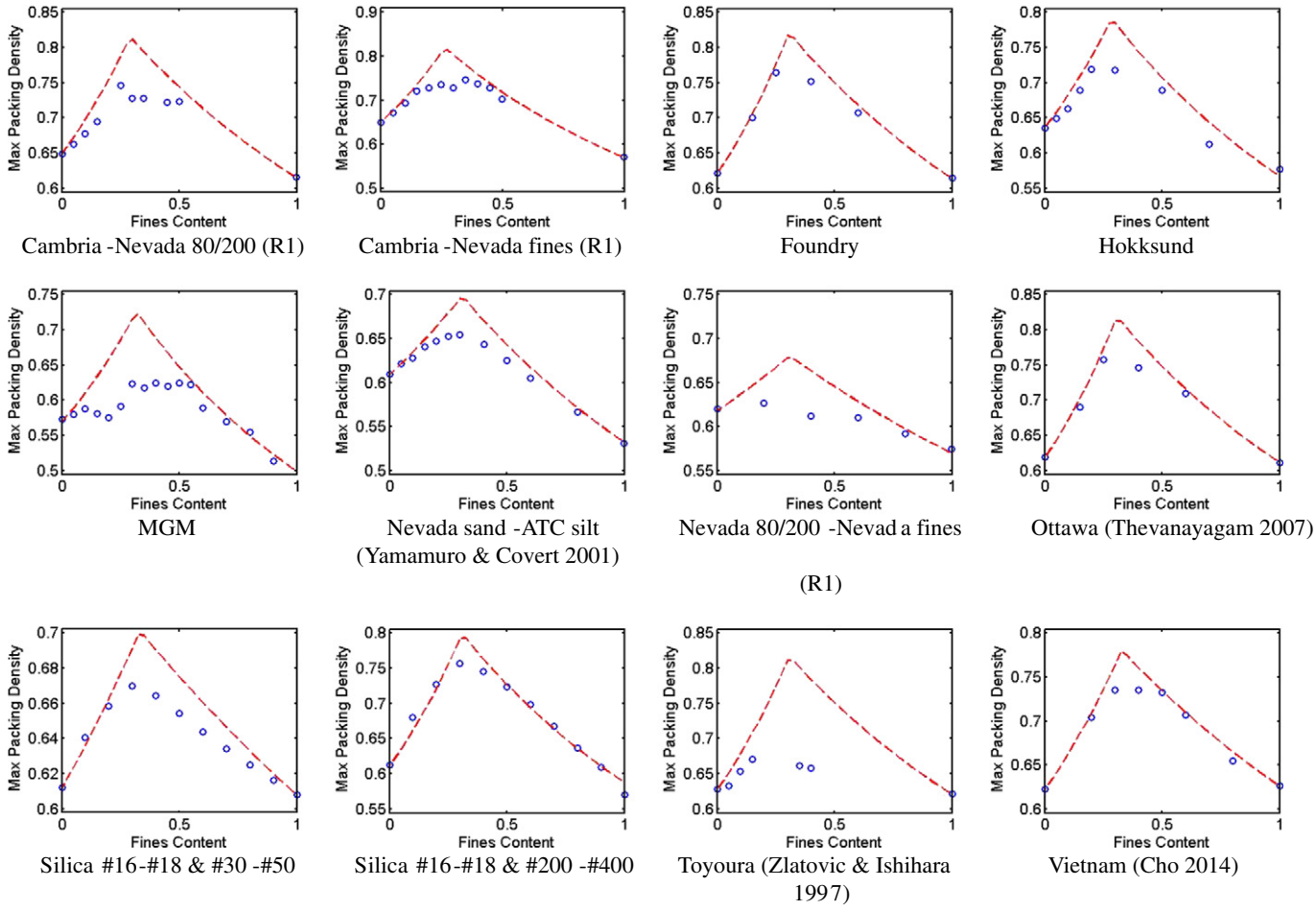

Fig. 4. Comparisons of predicted and measured maximum packing densities as functions of fines content.

The physical meaning of the assumption made by de Larrard is not easily seen. Furthermore, because of the linear nature of void ratio versus fines content (see Fig. 5), the material constant used in the present model can be straightforwardly determined from the experimental data as will be described later. Thus, we prefer to use void ratio as a variable in the present model.

Now, we consider a fine-grain dominant system. The phase diagram of a packing consisting of all fine particles is shown in Fig. 7a. Then, we consider the sand–silt mixture. The limiting situation is that all coarse particles are separate inclusions embedded in the matrix of fine-grain, and the void volume of the fine-grain matrix remains unchanged ($V_v = V_{v2}$, see Fig. 7b). Thus, the solid volume S1 is added to the total volume while the volume of V is kept to be the same as V2.

However, in a general case (see Fig. 7c), during the process of achieving minimum void ratio of the soil mixture, the void volume of fine grain matrix can be altered. Furthermore, if the content of coarse particles is large, the isolate coarse particles will tend to connect and be clustered, additional voids can be created between the coarse particles. Thus, the change of void volume, denoted as ΔV_v, is not null (see Fig. 7c). Note that $\Delta V_v = 0$ corresponds to the limiting situation.

The void ratio e^M of the mixture shown in Fig. 7c can be expressed as

$$e^M = \frac{V_{v2} + \Delta V_v}{V_{s1} + V_{s2}}. \tag{6}$$

Compared this void ratio of mixture e^M with the void ratio of pure silt e_2, the void ratio changes by two factors: (1) the void volume is changed due to the embedment phenomenon; and (2) the solid volume is increased to $V_{s1} + V_{s2}$. Observed from the phase diagrams, it is obvious that, after mixing of two components, the amount of void volume decrease due to filling phenomenon is much higher than that due to embedment phenomenon. Thus, the filling phenomenon has a greater effect on void ratio change with respect to a change of fines content.

In Chang and Meidani (2013), the void volume change is assumed to be proportional to the amount of sand added in the mixture, i.e., $\Delta V_v = \tilde{b} V_{s2}$. Note that $\tilde{b} = 0$ is corresponding to the limiting situation that there is no change of void volume during the process of achieving minimum void ratio of the soil mixture. Using this assumption, the minimum void ratio of the sand–silt mixture e^M in Eq. (6) can be written as a function containing e_2 and y_2:

$$e^M = e_2 y_2 + \tilde{b}(1 - y_2). \tag{7}$$

For a given fines content y_2, two values of minimum void ratio of the mixture, e^M, can be estimated, one from Eq. (5) and the other from Eq. (7). For the two values of e^M, the greater of the two values is likely to be achieved, because it requires less energy to reach the state. Thus, the greater of the two values is considered to be the solution.

Both Eqs. (5) and (7) show linear relationship between minimum void ratio and fines content. For the limiting case, $\tilde{a} = \tilde{b} = 0$, the line represented by Eq. (5) is shown in Fig. 8 as the line along AC, which intersects the vertical axis at $e = -1$ when the fines content is 1. Part of the line is below zero void ratio, it means that the amount of fines is greater than the available pore spaces of the coarse-grain network. Thus, this part of the line represents a physically invalid situation. The line represented by Eq. (7) is the line along CB, which goes through the point of zero void ratio when the fines content is 0. For each value of fines

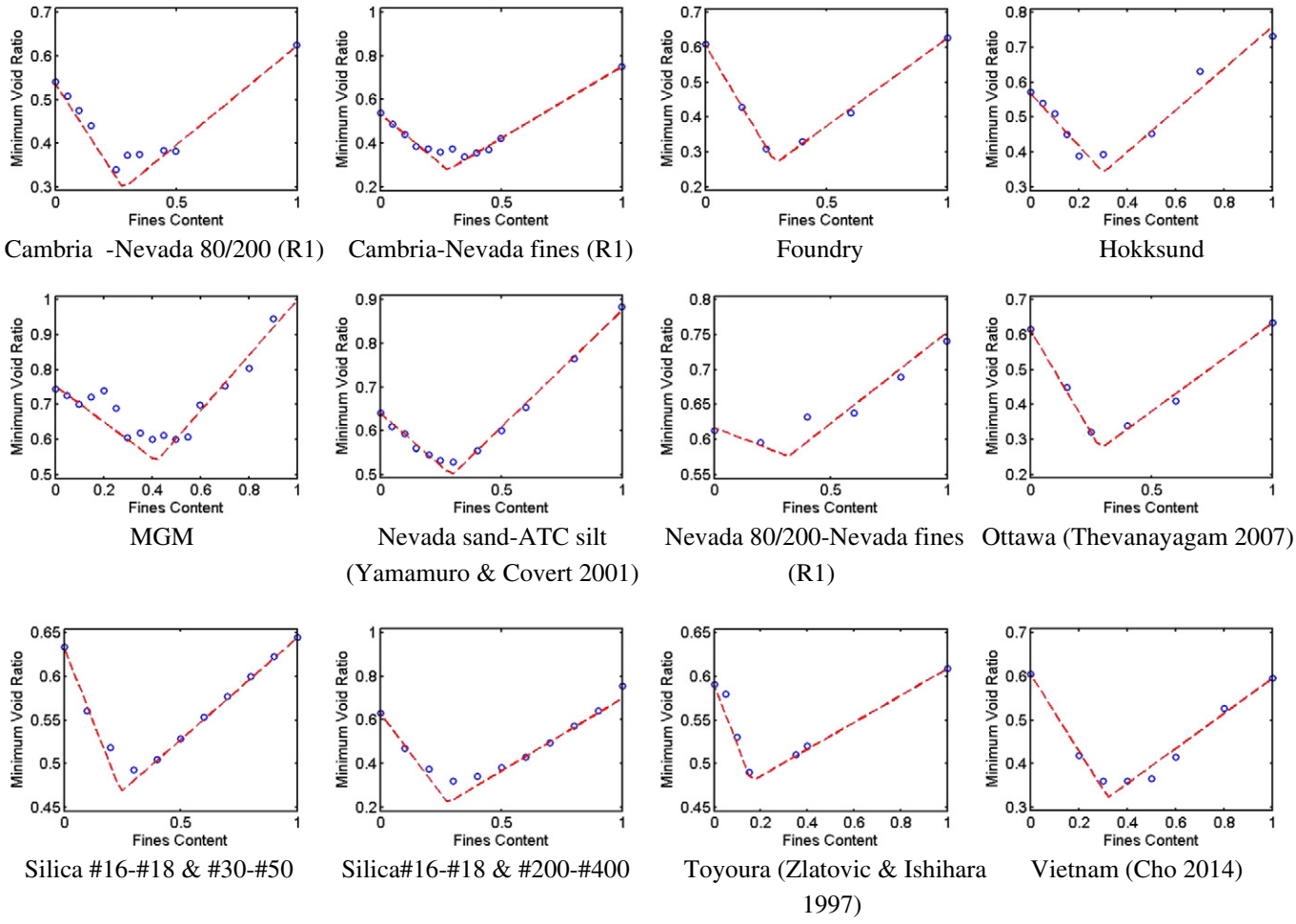

Fig. 5. Measured minimum void ratio versus fines content for some typical soil mixtures.

content, there is only one solution selected from Eqs. (5) and (7). The solid lines AC and CB are the selected solution, which gives the lower limit of the estimated minimum void ratio. In a general case where $\tilde{a}$ and $\tilde{b}$ are not equal to zero, the lines representing Eqs. (5) and (7) are located above the lower limit lines AC and CB.

In the lower limit case, by changing the notation of void ratio for the coarse grain network e_1 to e_c and fines content y_2 to f_c, Eq. (5) for the coarse grain dominant case can be rearranged to

$$e_c = \frac{e^M + f_c}{1 - f_c}. \tag{8}$$

The void ratio for the coarse grain network e_c can be estimated from the void ratio of the measured soil mixture e^M. The void ratio e_c is termed as skeleton void ratio by Mitchell (1993) and Vaid (1994), or inter-granular void ratio by Thevanayagam (2007). Similarly, Eq. (7) for the fine grain dominant case, can be rearranged to

$$e_f = \frac{e^M}{f_c}. \tag{9}$$

The void ratio corresponding to the fine grain network e_f is termed by Thevanayagam (2007) as inter-fine granular void ratio.

Observed from experimental data, the upper limit solution should be line AB as shown in Fig. 8. This line can be represented by the following equation:

$$e^M = e_1 y_1 + e_2 y_2. \tag{10}$$

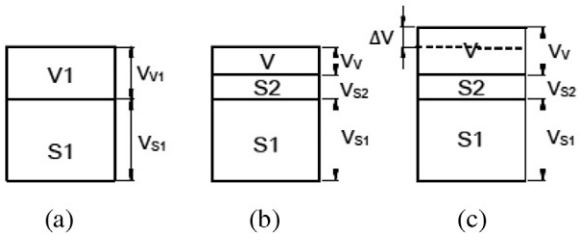

Fig. 6. Phase diagrams: (a) pure sand (before silt is added); (b) mixture (limiting case); (c) mixture (general case).

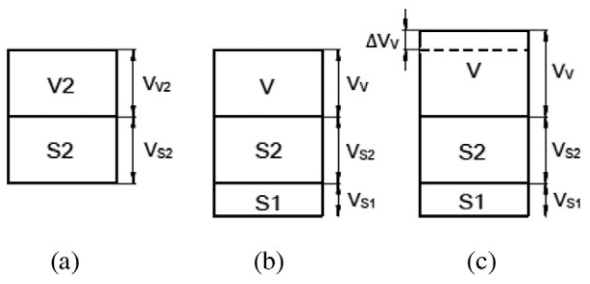

Fig. 7. Phase diagrams: (a) pure silt (before sand is added); (b) mixture (limiting case); (c) mixture (general case).

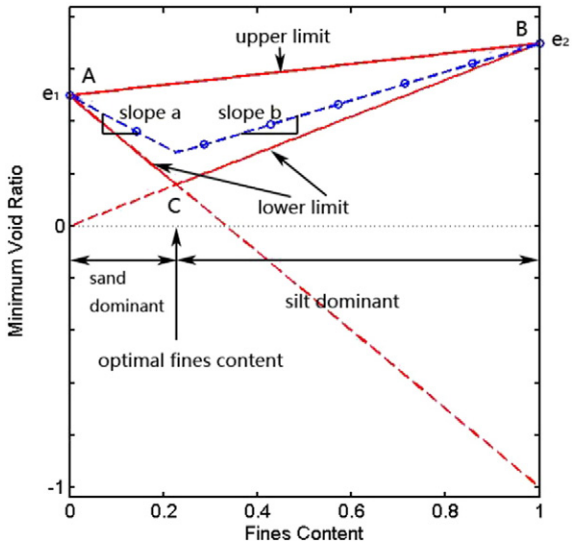

Fig. 8. Characteristics of void ratio versus fines content for a sand silt mixture.

It is noted that this equation is identical to the definition of volume average of the void ratios of the two components. The upper limit line is horizontal if $e_1 = e_2$.

The upper limit line AB and the lower limit lines, AC and CB, configure a triangular area. For a soil mixture, the measured minimum void ratios should be within this bounded area. Fig. 8 shows schematically the curve of minimum void ratios versus fines content within the triangular area. The slope for the left line is marked as slope_a, and the right one is marked as slope_b. These two lines, representing Eqs. (5) and (7), intersect at a point that gives the lowest value of minimum void ratio. Fines content corresponding to this point is termed optimum fines content. The value of optimum fines content can be solved from Eqs. (5) and (7), given by

$$(y_2)_{optimum} = \frac{e_1 - \tilde{b}}{1 + e_2 + e_1 - \tilde{a} - \tilde{b}}. \tag{11}$$

For packing with fines content less than the optimum, sand is the dominant component. Otherwise, the silt component dominates the system. For the limiting case, $\tilde{a} = \tilde{b} = 0$, the optimum point is C. The value of optimum fines content varies with the values of e_1 and e_2. When $e_1 = e_2$, point C locates at 33% fines content. The optimum fines content also varies, in a general case, with the values of $\tilde{a}$ and $\tilde{b}$. It is noted that, for the limiting case of Eq. (11), if the void ratio is converted to porosity and the fines content is converted from volume fraction definition to weight fraction definition, it can be shown that the optimum fines content and its corresponding porosity are identical to that proposed by Kezdi (1979) and Vallejo (2001). Thus, the solution obtained from the method proposed by Kezdi (1979) and Vallejo (2001) is corresponding to the lower limit bound of the present theory (i.e., the lines AC and CB shown in Fig. 8).

It is noted that the minimum void ratios for coarse grain e_1 and for fine grain e_2 usually do not have the same value. The experimental values of minimum void ratio (Table 1) are plotted against particle size in Fig. 9a. It shows that, in general, the value of minimum void ratio decreases with particle size. It is higher for silt than that for sand. This phenomenon may be caused by the difference in particle shapes. Silt particles are usually platy and angular whereas sand particles are usually sub-round to sub-angular and rotund in shape.

The ratio of e_2/e_1 against particle size ratio is plotted in Fig. 9b. Observed from experimental tests, the value of e_2/e_1 rages approximately from 0.8 to 1.4. The range of the minimum void ratio for sand is 0.5–0.63, and the range of the minimum void ratio for silt is 0.59–1.0.

Obtained from Eq. (5), the slope of AC in Fig. 8 is $-(1 + e_1)$. Obtained from Eq. (7), the slope of BC in Fig. 8 is e_2. Obtained from Eq. (10), the slope of AB in Fig. 8 is $(e_2 - e_1)$. These are the bounds of the slopes for the lines in a plot of void ratio versus fines content. For all the soil mixtures in Table 1, the bounds of slopes for fines content less than optimum (i.e., slope_a) is 0.24 to -1.63. For fines content greater than optimum, the bounds for slope_b are 0–1.

Both slope_a and slope_b of the experimental curves can be easily determined since they are linear in nature. The measured slopes for all the soil mixtures are listed in Table 1, and plotted by the circular symbols in Fig. 10. The values of measured slopes are within the computed bounds.

The average trends of slope_a and slope_b versus particle size ratio are marked as the solid lines in Fig. 10. For both slopes, the values are high (steep) at small particle size ratio d/D. With the increase of particle size ratio, both slopes decrease in value (i.e., becomes less steep). The value range of the particle size ratio is between 0 and 1.

It is noted that $\tilde{a} = \tilde{b} = 0$ corresponds to the lower limits. When $\tilde{a} = 1 + e_2$, the value of e^M in Eq. (5) is reduced to the upper limit of the minimum void ratio given in Eq. (10). Similarly, when $\tilde{b} = e_1$, Eq. (7) also becomes the upper limit Eq. (10). Thus, the value range of $\tilde{a}$ is between 0 and $1 + e_2$, and the value range of $\tilde{b}$ is between 0 and e_1. For convenience, the values of $\tilde{a}$ and $\tilde{b}$ can be normalized so that they are between 0 and 1. Let the two normalized constants be $a_{12} = 1 - \tilde{a}/(1 + e_2)$ and $b_{12} = 1 - \tilde{b}/e_1$, where the subscripts of a_{12} and b_{12} represent the interaction between size 1 and size 2 particles. Then Eqs. (5) and (7) can be rearranged as follows

$$e^M = e_1 y_1 + e_2 y_2 - a_{12}(1 + e_2) y_2 \tag{12}$$

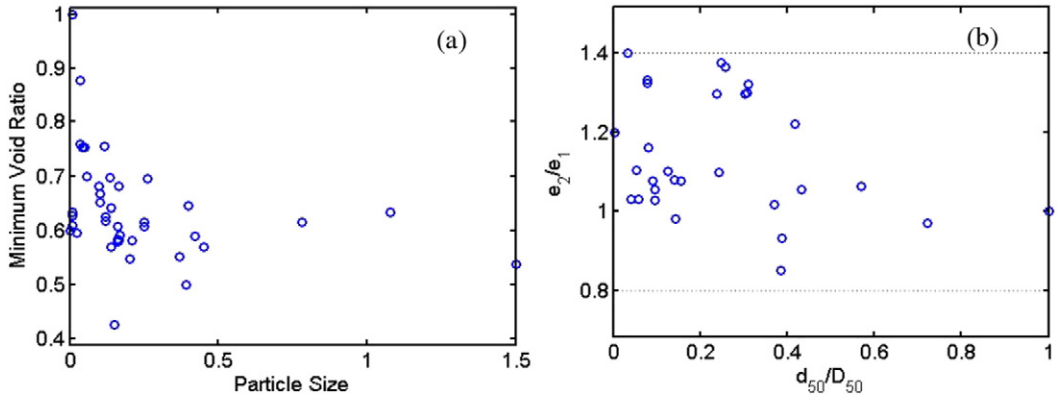

Fig. 9. (a) Minimum void ratio versus particle size and (b) ratio of minimum void ratio versus particle size ratio.

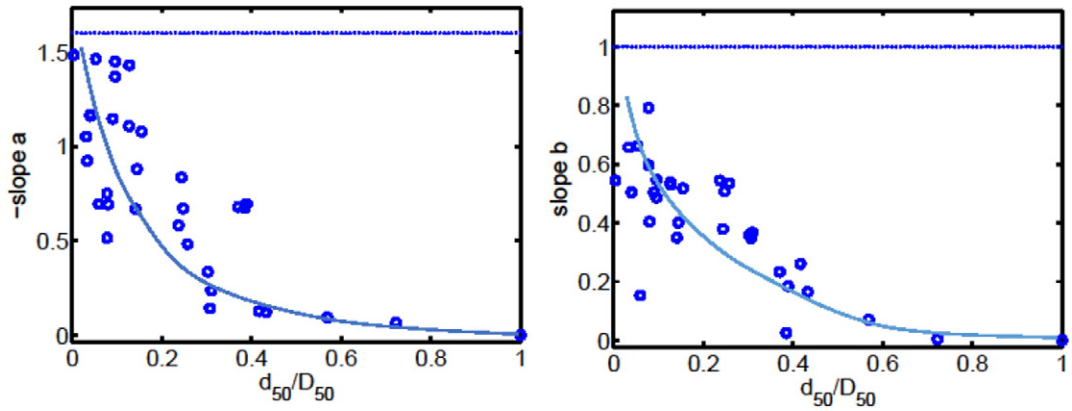

Fig. 10. Measured slopes from experimental results.

$$e^M = e_1 y_1 + e_2 y_2 - b_{12} e_1 y_1. \tag{13}$$

The values of both coefficients a_{12} and b_{12} are between 0 and 1. The parameter a_{12} is termed as filling coefficient. The case of $a_{12} = 1$ indicates that all fines can be filled into the voids without any distortion of the coarse grain network. This corresponds to the limiting case that the small particle size is extremely smaller than the size of large particles (i.e., d/D = 0). Another limiting case is $a_{12} = 0$, that corresponds to the limiting case that the size of small particles is almost the same as the size of large particles (i.e., d/D = 1), thus the small size particle cannot fit into the voids among large particles, and no "filling phenomenon" is present. For the particle size ratio between these two limits, the value of a_{12} is between 0 and 1.

The parameter of b_{12} is termed as embedment coefficient. The case of $b_{12} = 1$ indicates that the large particles are embedded in the fine grain matrix as isolated inclusions without any change of void volume of the fine grain matrix. This condition corresponds to the limiting case that the size of small particles is extremely smaller than the size of large particles (d/D = 0). Another limiting case is $b_{12} = 0$, that corresponds to the condition of size ratio d/D = 1. In this limiting case, the large particle size is the same as the size of the surrounding small particles. Thus, the "embedment" condition does not exist. For the particle size ratio between these two limits, the value of b_{12} is between 0 and 1.

By taking derivative of Eqs. (12) and (13), the constants, a_{12} and b_{12} can be expresses as follows:

$$a_{12} = \frac{e_2 - e_1}{1 + e_2} - \frac{1}{1 + e_2}\left(\frac{de^M}{dy_2}\right) \tag{14}$$

$$b_{12} = \frac{1}{e_1}\left(\frac{de^M}{dy_2}\right) - \frac{e_2 - e_1}{e_1}. \tag{15}$$

The term $\frac{de^M}{dy_2}$ in Eqs. (14) and (15) represents respectively the slope_a and slope_b schematically shown in Fig. 8. Both slopes can be easily determined directly from the experimental curves, thus the coefficients a_{12} and b_{12} can be easily obtained from Eqs. (14) and (15), which are listed in Table 1. When $e_2 = e_1$, the coefficients are directly proportional to the magnitude of slope. Thus, the physical meaning of a_{12} and b_{12} can be viewed as indices of slopes. Fig. 11 shows the values of a_{12} and b_{12} for all sand–silt mixtures listed in Table 1. The trends of the data points in Fig. 11 are similar to those in Fig. 10. But in Fig. 11, both the horizontal and vertical axes are within the bounds between 0 and 1.

Now, we select five Nevada sand–silt mixtures (see Table 1) as an example to further examine the value trend of coefficients a_{12} and b_{12}. Test results for four mixtures of Nevada sand with fines are obtained from the experimental work by Lade et al. (1998). In these four mixtures, the coarse particles are Nevada sand graded into four groups of different grain sizes. Each group of sand was mixed with fine particles. The fines are Nevada fines, which were obtained from natural Nevada sand passing through #200 sieve (with grains less than 0.075 mm). The shapes of sand grains were subangular to angular with increasing angularity with decreasing size. The minimum void ratios for the four mixtures were determined by a procedure similar to Japanese standard (see ref). Test results for the fifth mixture are from the work by Yamamuro and Covert (2001). In this mixture, the coarse particles are Nevada sand. The fines are ATC silt, which were primarily composed

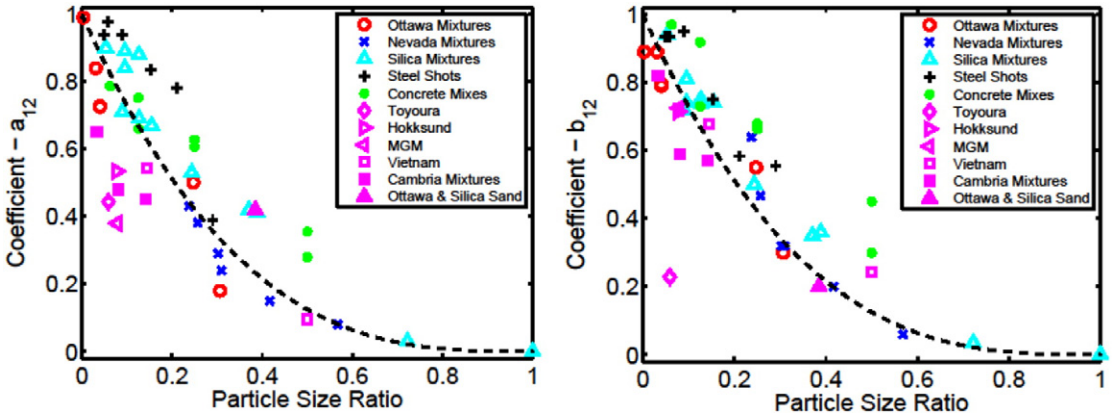

Fig. 11. Coefficients a_{12} and b_{12} determined from experimental results.

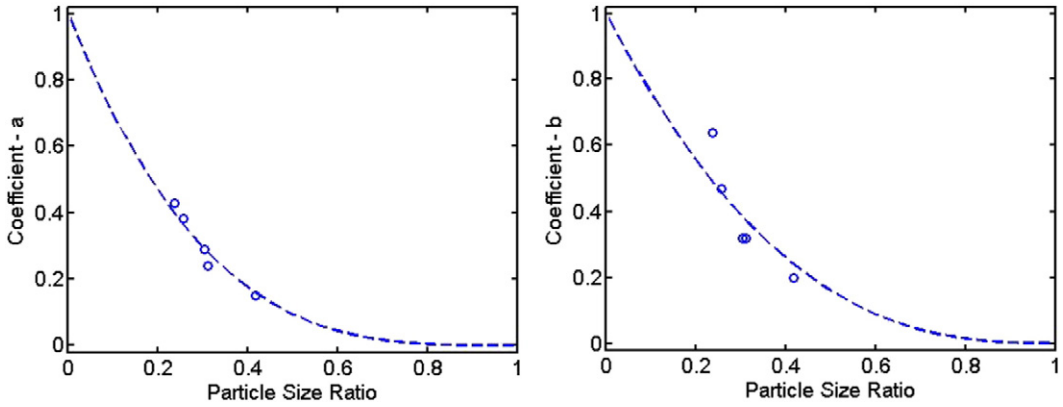

Fig. 12. Coefficients a_{12} and b_{12} for Nevada soil mixtures.

of quartz grains with insignificant amounts of mica fragments. The minimum void ratios for this soil mixture were determined by ASTM procedure (D4253).

As discussed in the previous section, the values of filling and embedment coefficients for soil mixture are influenced by both particle size ratio and shape characteristics. The five Nevada sand–silt mixtures consist of the same type of coarse grains and fines (except one mixture with ATC silt). Thus we expect that the particle shape characteristics of these five mixtures are similar, and the variations of filling and embedment coefficients are caused only by particle sizes.

The filling coefficients and embedding coefficients, a_{12} and b_{12}, for the five soil mixtures are plotted versus particle size ratio in Fig. 12. Data of both coefficients are fitted by a power function of particle size ratio, d_2/d_1, which accounts for the particle size effect between the coarse component 1 and the fine component 2, given by:

$$a_{12} = (1-d_2/d_1)^p \tag{16}$$

$$b_{12} = (1-d_2/d_1)^s. \tag{17}$$

For the two curves in Fig. 12, the value of the filling exponent $p = 3.41$ and the embedment exponent $s = 2.65$. We assume that for any sand–silt mixture, if their sand and silt particle shape characteristics are similar to those of Nevada soil mixtures, then their filling coefficients and embedding coefficients, a_{12} and b_{12}, can be predicted from the two values of exponents ($p = 3.41$, and $s = 2.65$) using Eqs. (16) and (17). Then, the minimum void ratio for the sand–silt mixture can be computed by Eqs. (12) and (13). Using $p = 3.41$, and $s = 2.65$, the predicted and measured void ratios versus fines content for the five Nevada mixtures are plotted in the left graph of Fig. 13. The steepest line is the soil mixture with ATC silt. The goodness of the prediction is shown in the right graph of Fig. 13.

It is noted that only two parameters, p and s, are required to predict the minimum void ratios of the five Nevada soil mixtures with various fines contents (59 individual samples). The predicted trends are in good agreement with the measured ones. The average discrepancy between predicted and measured void ratios is about 4%.

5. Evaluation of the new model

Besides Nevada sand–silt mixture, we evaluate the model using the experimental results for Silica sand–silt mixtures (Yilmaz, 2009, see Table 1) and for Ottawa sand–silt mixtures (Thevanayagam, 2007; Lade and Yamamuro, 1997; Pitman et al., 1994; Thevanayagam et al., 2002, see Table 1). Silica soil mixtures are made of commercially available Pasabahce silica sand, which is artificially graded using a variety of sieves into 12 subgroups with mean particle sizes (1.08 mm, 0.78 mm, 0.4 mm, 0.42 mm, 0.26 mm, 0.17 mm, 0.14 mm, 0.13 mm, 0.10 mm, 0.09 mm, 0.05 mm). The coarsest grains of size 1.08 mm are mixed individually with the other 11 subgroups. According to the USCS classification system, only the last group is in the silt category, the other 11 groups are classified as sand. Thus the mixtures are mainly sand–sand mixtures. The measured minimum void ratios were determined by the ASTM method for the 11 mixtures, which are shown in symbols in Fig. 14. This figure clearly shows the effect of particle size ratio on the slopes of these lines. The filling and embedment coefficients determined from test results are plotted in Fig. 15. For Silica soil mixtures, the filling exponent $p = 2.02$ and the embedment exponent $s = 2.27$. Using $p = 2.02$ and $s = 2.27$, the predicted minimum void ratios for the 11 mixtures are shown in dash-lines on the left graph of Fig. 14 while the goodness of the prediction is shown in the right

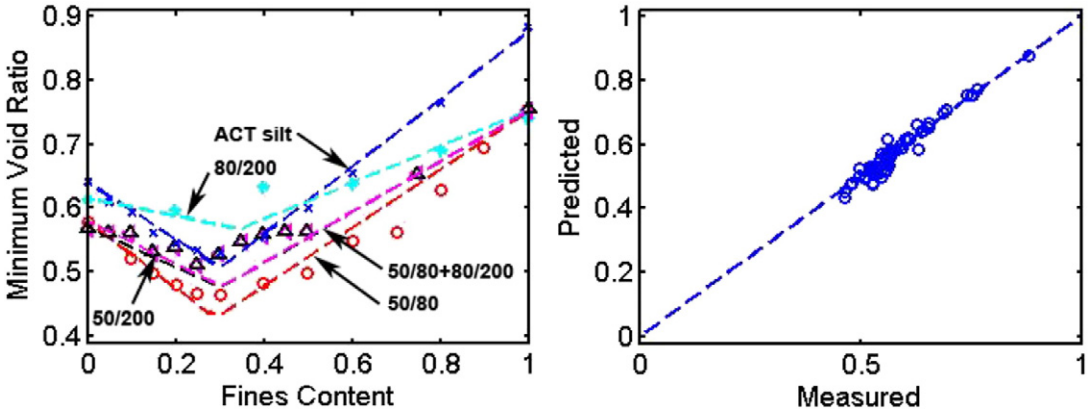

Fig. 13. Comparison of measured and predicted results for Nevada soil mixtures.

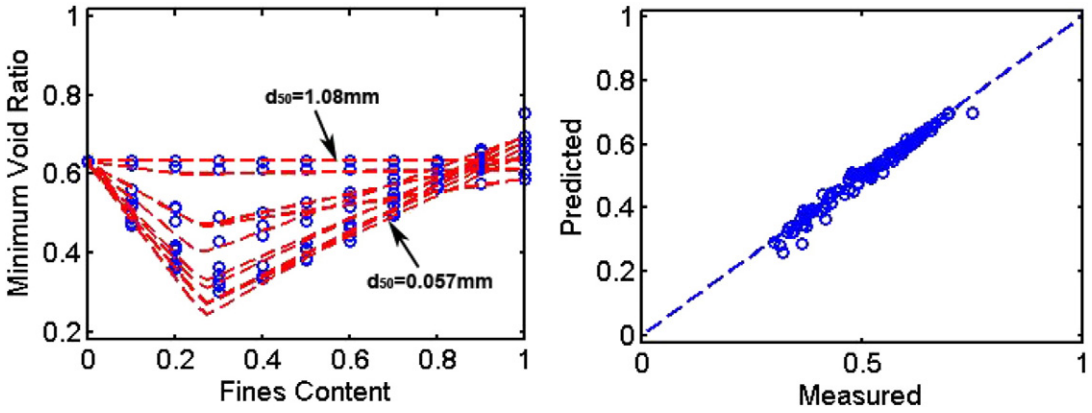

Fig. 14. Comparison of measured and predicted results for Silica soil mixtures.

graph of Fig. 14. In this case, it requires only two parameters, p and s, to predict the minimum void ratios of the 11 Silica soil mixtures with various fines contents (120 individual samples). The predicted trends are in good agreement with the measured ones. The average discrepancy between predicted and measured void ratios is about 2%.

There are five types of Ottawa sand–silt mixtures selected. In all five mixtures, the coarse particles are Ottawa sand of different sizes. However, for these mixtures, there are three types of fines: the Nevada fines (Lade et al., 1998), and the silica fines (Thevanayagam, 2007; Pitman et al., 1994), and the Kaolinite fines (Pitman et al., 1994). Because the fines are not of the same type, thus their particle shape character may not be same. Methods of determining minimum void ratios for these mixtures were ASTM and modified Japanese standard. The measured minimum void ratios for the five mixtures are shown in symbols in Fig. 16. The coefficients, a_{12} and b_{12}, determined from test results are shown in Fig. 15. The filling exponent $p = 3.86$ and the embedment exponent $s = 2.89$. Using $p = 3.86$ and $s = 2.89$, the predicted minimum void ratios for the five mixtures are shown in dash-lines on the left graph of Fig. 16. The goodness of the prediction is shown in the right graph of Fig. 16. The line represents C109 Ottawa sand with silica fines (marked as C109-S in Fig. 16), did not have enough test results to cover all range of fines content. The soil mixture with Kaolinite fines (marked as C109-K) gives the lowest void ratios. For the five Ottawa soil mixtures with various fines contents (54 individual samples), the predicted trends are in good agreement with the measured ones. The average discrepancy between predicted and measured void ratios is about 3%.

For purpose of comparison, the minimum void ratios of steel shots (McGeary, 1961, see Fig. 1) and concrete mixes (data from de Larrard, 1999) are also included in the analysis. The values of coefficients, a_{12} and b_{12}, were determined from test results and plotted versus particle size ratio given in Fig. 15. For steel shots, the filling exponent $p = 1.20$, and the embedment exponent $s = 1.76$; and for gravel and sand mixes used in concrete, the filling exponent $p = 1.82$, and the embedment exponent $s = 1.40$.

Viewing the particle shape information from Table 1, Silica soil mixtures consist of subangular sand and subangular silt. Nevada soil mixtures consist of subangular-to-angular sand and angular silt. Ottawa soil mixtures consist of subround sand and angular silt. Concrete mixes consist of subround aggregate and subround sand. The steel shots are very close to spherical shape for both sizes of particles. For the abovementioned five sets of particle mixtures, we can classify them into two categories: (1) the coarse grains and fine grains are of the same shape (steel shots, concrete mixes and Silica soil mixtures), and (2) the coarse grains and fine grains are of different shapes (Nevada soil mixture and Ottawa soil mixture).

The values of exponents of the first category mixtures, p and s, are smaller than those of the second category mixtures. Smaller values of exponents imply smaller curvatures of the curves. That means the rates of change of a_{12} and b_{12} are nearly constant with respect to the change of particle size ratio. Larger values of exponents means the rates of change of a_{12} and b_{12} vary depending on the particle size ratio. For soil mixtures within the first category, the exponents seem to increase with the particle angularity, in the order of steel shots, concrete mixes and Silica soil mixtures. The only exception is the embedment exponents for steel shots and concrete mixes.

For soil mixtures within the second category, the exponents of the Nevada soil mixture are smaller than those of the Ottawa soil mixture. We may observe that the exponents are smaller when there is a less contrast of dissimilarity between the coarse and fine particle shapes for the soil mixtures. The Ottawa soil mixture has a more contrast of dissimilarity between its subround sand and angular silt, than the

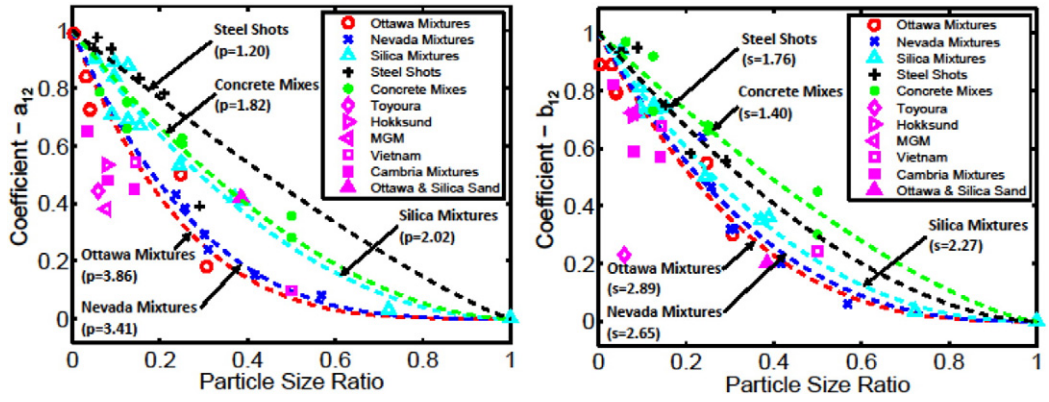

Fig. 15. Coefficients a_{12} and b_{12} for 31 soil mixtures listed on Table 1.

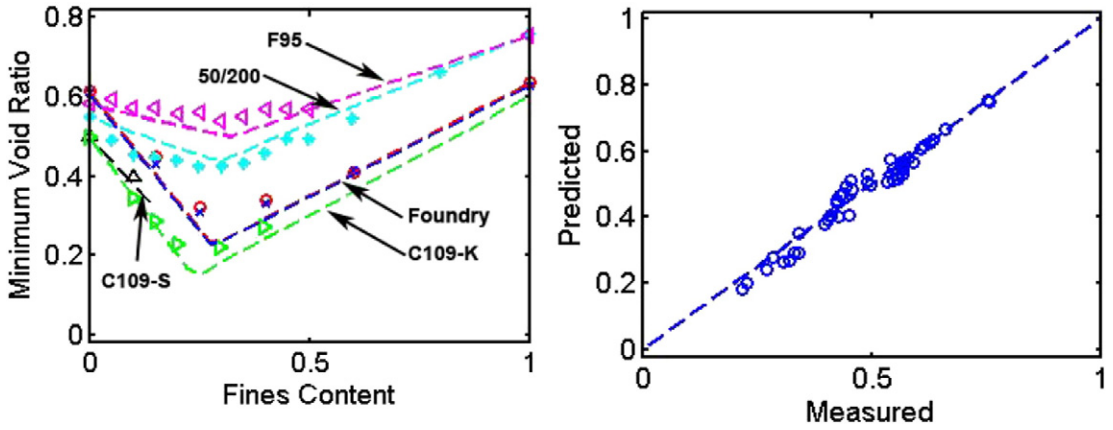

Fig. 16. Comparison of measured and predicted results for Ottawa soil mixtures.

dissimilarity of the Nevada soil mixture, which consists of subangular-to-angular sand and angular silt.

Besides the soil mixtures mentioned above, there are a few other soil mixtures in Table 1. There are 3 Cambria mixtures, 2 Vietnam mixtures, and 4 individual mixtures: Toyoura, Hokksund, MGM, and Ottawa & Silica sands. These soil mixtures do not contain mixtures of several particle size ratios, thus are not suitable to be used directly for studying the particle size effect. However, their filling and embedment coefficients for these individual tests were also determined from test results and included in Fig. 15. Their corresponding exponents were computed. For all soil mixtures, the overall range of $s = 2$–6, and the range of $p = 2$–7.

In the three Cambria mixtures, two of them are mixed with Nevada sand (sand–sand mixtures), and one of them is mixed with Nevada fines (sand–silt mixture). The particle shape is round for Cambria sand, subangular-to-angular for Nevada sand, and angular for Nevada fines. For the three Cambria mixtures, the contrast of dissimilarity between coarse and fine particle shapes is more than that of the five Ottawa mixtures analyzed in previous section (i.e. subround sand and angular silt). Thus it is reasonable that their exponents are higher than those of Ottawa soil mixtures.

In the two Vietnam soil mixtures, one is sand–sand mixture and the other is sand–silt mixture. Both sands and fines are subangular in shape. The particle shape characteristics are similar to those of the five Nevada mixtures (i.e. subangular-to-angular sand, and angular silt). Thus the values of exponents, as expected, are close to Nevada sand.

For Toyoura soil mixture, the particles are elongated, and the milled fines are highly angular. Thus, the contrast of dissimilarity between sand and fines is very large. The values of exponents are very high as shown in Fig. 15. The Hokksund soil mixture consists of Hokksund sand and Chengbei silt. The shape of Hokksund sands is cubical/rotund in shape, and the shape of Chengbei silt is angular. The shape contrast of dissimilarity between coarse and fine particles is similar to that of Cambria soil mixture, thus the values of exponents are close to the Cambria soil mixtures as shown in Fig. 15. For MGM (Merriespruit gold mining tailing), the coarse tailing sand consists of highly angular to sub-rounded bulky but flattened particles. The finer slimes consist of mostly of thin plate-like particles. Because of the large contrast of dissimilarity between the coarse and fine particle shapes, the values of exponents are expected to be high as shown in Fig. 15. The mixture of Ottawa and silica sands, is a sand–sand mixture, thus it was not included in the Ottawa sand–silt mixtures group analyzed previously. In this mixture, both Ottawa and Silica sands are subround in shape, thus it is not surprising that the filling exponent is almost identical to that of concrete mixes. However, the embedment exponent is close to that of Ottawa soil mixture.

During either filling or embedment phenomenon, the change of minimum void ratio with respect to the particle size ratio is likely to be more sensitive for mixtures with higher contrast of dissimilarity in particle shapes. This explanation seems to be in agreement with the test results for most soil mixtures listed in Table 1, based on the available qualitative descriptions of particle shapes.

It is noted that the natural sand–silt mixtures are much more deviated in particle shapes than concrete mixes or other types of industrial material. Therefore, it is not realistic to have a universal equation. It is more practical to model the behavior of soil with different parameters of p and s. Fig. 15 gives a guide for the estimation of values of p and s based on particle shapes of soil mixtures.

6. Conclusion

A new model is proposed that can better predict the minimum void ratios for sand–silt mixtures with different particle sizes. This proposed model requires only two parameters, p and s, for the prediction of minimum void ratios of soil mixtures with various fines contents. Using two parameters, the minimum void ratios of Silica soil mixtures (120 individual samples of various fines contents) were predicted and compared with measured results. The predicted trends are in good agreement with the measured ones. The average discrepancy between predicted and measured void ratios is about 2%. The comparisons of the predicted and measured results for Nevada soil mixtures and Ottawa soil mixtures also show that the model is suitable for predicting minimum void ratios of sand–silt mixtures.

The values of parameters, p and s, for Silica soil mixtures are different from those for Nevada soil mixtures and for Ottawa soil mixtures. It is obvious that these two parameters are related to the particle shape characteristics of the constituents of soil mixtures (i.e. sand and silt). However, at the present stage, both analytical methods and experimental data on quantitative descriptions for soil particle shapes are lacking in the literature. Thus, this type investigation will be for future work.

Acknowledgment

Financial support from the Ministry of Science and Technology, Taiwan (MOST), project number 103-2811-E-002-026 is greatly appreciated.

References

AASHTO, 1986. Correction for coarse particles in the soil compaction test. AASHTO Designation: T224-86pp. 840–845.
Aberg, B., 1992. Void ratio of noncohesive soils and similar materials. ASCE J. Geotech. Eng. 118 (9), 1315–1334.
An, X.Z., 2013. Densification of the packing structure under vibrations. Int. J. Miner. Metall. Mater. 20 (5), 499–504. http://dx.doi.org/10.1007/s12613-013-0757-9 (May).
Ben Aim, R., Le Goff, P., 1967. Effect de Paroi Dans Les Empilements Desordonnes de Spheres et Application aa La Porosite de Melanges Binaires. Powder Technol. 1, 281–290.
Bobei, D.C., Lo, S.R., Wanatowski, D., Gnanendran, C.T., Rahman, M.M., 2009. A modified state parameter for characterizing static liquefaction of sand with fines. Can. Geotech. J. 46 (3), 281–295.

Chang, C.S., Meidani, M., 2013. Dominant grains network and behavior of sand–silt mixtures: stress–strain modeling. Int. J. Numer. Anal. Methods Geomech. 37, 2563–2589.
Cho, Y.T., 2014. The Study of GCTS Triaxial Apparatus Function and Mixing Sand Void Ratio (Master Thesis) Department of Civil Engineering, National Taiwan University.
Cho, G.C., Dodds, J., Santamarina, J.C., 2006. Particle shape effects on packing density, stiffness, and strength: natural and crushed sands. J. Geotech. Geoenviron. Eng. ASCE 132 (5), 591–602.
Cubrinovski, M., Ishihara, K., 2002. Maximum and minimum void ratio characteristics of sand. Soils Found. 42 (6), 65–78.
De Larrard, F., 1999. Concrete Mixture Proportioning: A Scientific Approach. Taylor & Francis, London (1999).
Fennis, S.A.A.M., Walraven, J.C., den Uijl, J.A., 2013. Compaction-interaction packing model: regarding the effect of fillers in concrete mixture design. Mater. Struct. 46 (3), 463–478.
Fourie, A.B., Papageorgiou, G., 2001. Defining an appropriate steady state line for Merriespruit gold tailings. Can. Geotech. J. 38, 695–706.
Fragaszy, R.J., Sneider, C.A., 1991. Compaction control of granular soils. Final Report WA-RD 230.1. Washington State Department of Transportation.
Fuggle, A., Roozbahani, M., Frost, J., 2014. Size effects on the void ratio of loosely packed binary particle mixtures. Geo-Congress 2014 Technical Papers, pp. 129–138. http://dx.doi.org/10.1061/9780784413272.014.
Humphres, H.W., 1957. A method for controlling compaction of granular materials. Highw. Res. Board Bull. 159, 41–57.
Kezdi, A., 1979. Soil physics: selected topics. Elsevier Scientific Co, Amsterdam (160 pp.).
Kolbuszewski, J.J., 1948. An experimental study of the maximum and minimum properties of sands. Proceedings, Second International Conference in Soil Mechanics and Foundation Engineering, Rotterdam vol. 1, pp. 158–165.
Kwan, A.K.H., Fung, W.W.S., 2009. Packing density measurement and modeling of fine aggregates and mortar. Cem. Concr. Compos. 31, 349–357.
Lade, P.V., Yamamuro, J., 1997. Effects of nonplastic fines on static liquefaction of sands. Can. Geotech. J. 34 (6), 917–928.
Lade, P.V., Liggio Jr., C.D., Yamamuro, J.A., 1998. Effects of non-plastic fines on minimum and maximum void ratios of sand. Geotech. Test. J. 21 (4), 336–347.
McGeary, R.K., 1961. Mechanical packing of spherical particles. J. Am. Ceram. Soc. 44 (10), 513–522.
Mitchell, J.K., 1993. Fundamentals of Soil Behavior. 2nd edn. Wiley Interscience Publ.
Miura, K., Maeda, K., Furukawa, Toki, S., 1997. Physical characteristics of sands with different primary properties. Soils Found. 37 (3), 53–64.
Mulilis, J.P., Seed, H.B., Chan, C.K., Mitchell, J.K., Arulanandan, K., 1977. Effect of sample preparation on soil liquefaction. J. Geotech. Eng. Div. 103 (GT2), 91–108.
Peters, J.F., Berney, E.S., 2010. Percolation threshold of sand–clay binary mixtures. J. Geotech. Geoenviron. Eng. 136 (2), 310–318.
Pitman, T.D., Robertson, P.K., Sego, D.C., 1994. Influence of fines on the collapse of loose sands. Can. Geotech. J. 31 (5), 728–739.
Powers, T.C., 1968. The Properties of Fresh Concrete. John Wiley & Sons, New York.
Reed, J.S., 1995. Principles of Ceramics Processing. 2nd ed. John Wiley & Sons, New York.
Selig, E.T., Ladd, R.S., 1973. Evaluation of relative density measurements and applications. Evaluation of Relative Density and Its Role in Geotechnical Projects Involving Cohesionless SoilsASTM STP 523 pp. 487–504.
Smith, L.N., 2003. A Knowledge-based System for Powder Metallurgy Technology. Professional Engineering Publishing Ltd, London and Bury St. Edmunds.
Stovall, T., De Larrard, F., Buil, M., 1986. Linear packing density model of grain mixtures. Powder Technol. 48 (1), 1–12.
Thevanayagam, S., 2007. Intergrain contact density indices for granular mixes — I: framework. Earthq. Eng. Eng. Vib. 6 (2), 123–134.
Thevanayagam, S., Shenthan, T., Mohan, S., Liang, J., 2002. Undrained fragility of clean sands, silty sands and sandy silts. ASCE J. Geotech. Geoenviron. Eng. 128 (10), 849–859.
Vaid, Y.P., 1994. Liquefaction of silty soils. Proceedings of Ground Failures Under Seismic ConditionsGeotechnical Special Publication 44. ASCE, New York, pp. 1–16.
Vaid, Y.P., Negussey, D., 1988. Preparation of reconstituted sand specimens. In: Donaghe, R.T., Chaney, R.C., Silver, M.L. (Eds.), Advance Triaxial Testing of Soil and Rock. American Society for Testing and Materials, West Conshohocken, PA, pp. 405–417 (ASTM STP 977).
Vallejo, L.E., 2001. Interpretation of the limits in shear strength in binary granular mixtures. Can. Geotech. J. 38, 1097–1104.
Westman, A.E.R., Hugill, H.R., 1930. The packing of particles. J. Am. Ceram. Soc. 13 (10), 767–779.
Yamamuro, J.A., Covert, K.M., 2001. Monotonic and cyclic liquefaction of very loose sands with high silt content. ASCE J. Geotech. Geoenviron. Eng. 127 (4), 314–324.
Yang, S.L., 2004. Characterization of the Properties of Sand–Silt Mixtures (Ph.D. dissertation) Norwegian University of Science and Technology, Trondheim, Norway.
Yilmaz, Y., 2009. A study on the limit void ratio characteristics of medium to fine mixed graded sands. Eng. Geol. 104, 290–294.
Yilmaz, Y., Mollamahmutoglu, M., Ozaydin, V., Kayabali, K., 2008. Experimental investigation of the effect of grading characteristics on the liquefaction resistance of various graded sands. Eng. Geol. 100, 91–100.
Yu, A.B., Standish, N., 1987. Porosity calculations of multi-component mixtures of spherical particles. Powder Technol. 52 (3), 233–241.
Zlatovic, S., Ishihara, K., 1997. Normalized behavior of very loose non-plastic soils: effects of fabric. Soils Found. 37 (4), 47–56.